

DTIC FILE COPY

WRDC-TR-90-2078



WEAR MEASUREMENT OF CERAMIC BEARINGS IN GAS TURBINES

A.J. Armini, Ph.D.
S.N. Bunker, Ph.D.

AD-A227 505

IMPLANT SCIENCES CORPORATION
35 CHERRY HILL DRIVE
DANVERS, MA 01923

MARCH 1990

Final Report for Period August 1989 - March 1990

APPROVED FOR PUBLIC RELEASE; DISTRIBUTION IS UNLIMITED.



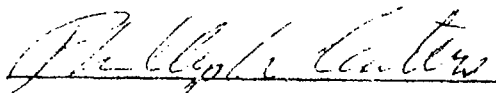
AERO PROPULSION AND POWER LABORATORY
WRIGHT RESEARCH AND DEVELOPMENT CENTER
AIR FORCE SYSTEMS COMMAND
WRIGHT-PATTERSON AIR FORCE BASE, OHIO 45433-6523

NOTICE

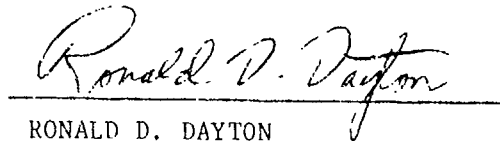
WHEN GOVERNMENT DRAWINGS, SPECIFICATIONS, OR OTHER DATA ARE USED FOR ANY PURPOSE OTHER THAN IN CONNECTION WITH A DEFINITELY GOVERNMENT-RELATED PROCUREMENT, THE UNITED STATES GOVERNMENT INCURS NO RESPONSIBILITY OR ANY OBLIGATION WHATSOEVER. THE FACT THAT THE GOVERNMENT MAY HAVE FORMULATED OR IN ANY WAY SUPPLIED THE SAID DRAWINGS, SPECIFICATIONS, OR OTHER DATA, IS NOT TO BE REGARDED BY IMPLICATION, OR OTHERWISE IN ANY MANNER CONSTRUED, AS LICENSING THE HOLDER, OR ANY OTHER PERSON OR CORPORATION; OR AS CONVEYING ANY RIGHTS OR PERMISSION TO MANUFACTURE, USE, OR SELL ANY PATENTED INVENTION THAT MAY IN ANY WAY BE RELATED THERETO.

THIS REPORT HAS BEEN REVIEWED BY THE OFFICE OF PUBLIC AFFAIRS (ASD/PA) AND IS RELEASABLE TO THE NATIONAL TECHNICAL INFORMATION SERVICE (NTIS). AT NTIS IT WILL BE AVAILABLE TO THE GENERAL PUBLIC INCLUDING FOREIGN NATIONS.

THIS TECHNICAL REPORT HAS BEEN REVIEWED AND IS APPROVED FOR PUBLICATION.

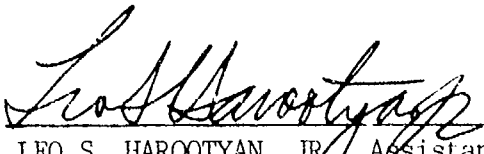


PHILLIP W. CENTERS, PhD, TAM
Lubrication Branch
Fuels and Lubrication Division
Aero Propulsion and Power Laboratory



RONALD D. DAYTON
Actg Chief, Lubrication Branch
Fuels and Lubrication Division
Aero Propulsion and Power Laboratory

FOR THE COMMANDER



LEO S. HAROOTYAN, JR., Assistant Chief
Fuels and Lubrication Division
Aero Propulsion and Power Laboratory

IF YOUR ADDRESS HAS CHANGED, IF YOU WISH TO BE REMOVED FROM OUR MAILING LIST, OR IF THE ADDRESSEE IS NO LONGER EMPLOYED BY YOUR ORGANIZATION PLEASE NOTIFY WRDC/POSL, WRIGHT-PATTERSON AFB, OH 45433-6563 TO HELP MAINTAIN A CURRENT MAILING LIST.

COPIES OF THIS REPORT SHOULD NOT BE RETURNED UNLESS RETURN IS REQUIRED BY SECURITY CONSIDERATIONS, CONTRACTUAL OBLIGATIONS, OR NOTICE ON A SPECIFIC DOCUMENT.

REPORT DOCUMENTATION PAGE				Form Approved OMB No. 0704-0188	
1a. REPORT SECURITY CLASSIFICATION UNCLASSIFIED			1b. RESTRICTIVE MARKINGS NONE		
2a. SECURITY CLASSIFICATION AUTHORITY			3. DISTRIBUTION/AVAILABILITY OF REPORT Approved for public release; distribution unlimited.		
2b. DECLASSIFICATION/DOWNGRADING SCHEDULE					
4. PERFORMING ORGANIZATION REPORT NUMBER(S)			5. MONITORING ORGANIZATION REPORT NUMBER(S) WRDC-TR-90- 2078		
6a. NAME OF PERFORMING ORGANIZATION Implant Sciences Corporation		6b. OFFICE SYMBOL (If applicable)	7a. NAME OF MONITORING ORGANIZATION Wright Research & Development Center Aero Propulsion & Power Laboratory (WRDC/POSL)		
6c. ADDRESS (City, State, and ZIP Code) 35 Cherry Hill Drive Danvers, MA 01923			7b. ADDRESS (City, State, and ZIP Code) Wright-Patterson AFB OH 45433-6563		
8a. NAME OF FUNDING, SPONSORING ORGANIZATION		8b. OFFICE SYMBOL (If applicable)	9. PROCUREMENT INSTRUMENT IDENTIFICATION NUMBER Contract No. F33615-89-C-2942		
8c. ADDRESS (City, State, and ZIP Code)			10. SOURCE OF FUNDING NUMBERS		
			PROGRAM ELEMENT NO. 65502F	PROJECT NO. 3005	TASK NO. 21
					WORK UNIT ACCESSION NO. 52
11. TITLE (Include Security Classification) Wear Measurement of Ceramic Bearings in Gas Turbines					
12. PERSONAL AUTHOR(S) A. J. Armini abd S. N. Bunker					
13a. TYPE OF REPORT Final Report		13b. TIME COVERED FROM 8/89 TO 3/90		14. DATE OF REPORT (Year, Month, Day) 1990 March	
15. PAGE COUNT 57					
16. SUPPLEMENTARY NOTATION					
17. COSATI CODES			18. SUBJECT TERMS (Continue on reverse if necessary and identify by block number) Wear Analysis, Activation, Turbine Engines SiN		
FIELD	GROUP	SUB-GROUP			
11	08				
14	02				
19. ABSTRACT (Continue on reverse if necessary and identify by block number) The objective of this program was to determine the feasibility of measuring ceramic bearing wear in real time. The method chosen is to selectively introduce a radioactive tag into the surface of a ceramic part and to measure the wear amount by monitoring the strength of the tagging activity as the test progresses. Although this method has been used for many years in the automobile and heavy machinery industries, it has not yet been used to measure the extremely minute amounts of wear which are experienced by ball bearings. This program was analytical in nature, and its principal task was to show the feasibility and accuracy of such a technique applied to SiN ₄ and SiC ceramic bearing components. In addition the goal was to develop the analytical theory and operational techniques needed for wear tests. <div style="text-align: right;">(continued on reverse)</div>					
20. DISTRIBUTION/AVAILABILITY OF ABSTRACT <input checked="" type="checkbox"/> UNCLASSIFIED/UNLIMITED <input type="checkbox"/> SAME AS RPT. <input type="checkbox"/> DTIC USERS			21. ABSTRACT SECURITY CLASSIFICATION UNCLASSIFIED		
22a. NAME OF RESPONSIBLE INDIVIDUAL ROBERT L. WRIGHT			22b. TELEPHONE (Include Area Code) (513) 255-3551		22c. OFFICE SYMBOL WRDC/POSL

The primary findings of the program are:

a. The method for tagging Si_3N_4 , SiC , and M50 bearing components to depths of interest in bearings (1-20 microns) was developed.

b. Calculated techniques were developed to predict activation and count rates in the detector system for both the pin-on-disk and bearing test rig.

c. The data acquisition electronics were selected.

d. Radiation safety issues were examined and found to be not a problem since activity levels required were below values exempt from regulation by the NRC or the States.

e. The use of the technique was deemed feasible and useful for measuring needed wear parameters in materials under conditions important to ceramic bearing operation.

Accession By	
NTIS GRA&I	<input checked="" type="checkbox"/>
DTIC TAB	<input type="checkbox"/>
Unannounced	<input type="checkbox"/>
Justification	
By	
Distribution/	
Availability Codes	
Dist	Avail and/or Special
A-1	

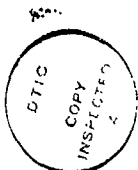


TABLE OF CONTENTS

<u>Section</u>	<u>Page</u>
1 INTRODUCTION	1-1
2 BACKGROUND	3-1
3 SELECTION OF BEARING WEAR EXPERIMENTS	3-1
3.1 Pin-on-Disk Tests	3-2
3.1.1 Pin-on-Disk Test Geometry	3-6
3.2 High Speed Bearing Rig Tests	3-8
4 DETERMINATION OF NUCLEAR TAGGING METHODS AND DETECTION	4-1
4.1 Direct Nuclear Reaction Method	4-1
4.2 The Recoil Implantation Method	4-4
5 DATA ACQUISITION SYSTEM	5-1
6 CALIBRATION TECHNIQUES	6-1
7 RADIATION SAFETY CONSIDERATIONS	7-1
8 CONCLUSION AND RECOMMENDATIONS	8-1
REFERENCES	REF-1
Appendix A - Calculation of Expected Count Rates in Detector	A-1
Appendix B - Calculation of Recoil Implanted Activity Versus Depth	B-1

LIST OF ILLUSTRATIONS

<u>Figure</u>		<u>Page</u>
2-1	Original Application of the SLA technique to nosetip erosion during re-entry	2-3
2-2	Piston ring activation of a thin surface layer showing the activation depth profile	2-3
2-3	Outside race in operating position being continuously monitored by a gamma ray detector outside of a turbopump engine	2-4
3-1	Photograph of Implant Sciences' pin-on-disk tested with ceramic ball on M50 disk.	3-3
3-2	Diagram of Implant Sciences' pin-on-disk tester (top view)	3-3
3-3	Ball bearing on flat disk. Left side before test, right side after groove worn	3-6
3-4	Schematic of stationary roller (pin) on SLA activated ring (disk)	3-7
3-5	Inner ring heat generation and Hertz stress as a function of inner ring conformity and contact angle	3-9
3-6	Schematic of typical bearing test rig and Gamma ray detector in position	3-10
4-1	Geometry for calculation of count rate in pin-on-disk	4-3
4-2	Geometry used during activation by recoil implantation of Be	4-4
4-3	Spectrum of Be ⁷ nuclear generated by inelastic recoil reaction	4-5
4-4	Calculation of depth profile of each energy bin of Be ⁷ recoils in M50	4-6
5-1	Typical calibration curve in SLA wear test	5-2
5-2	Block diagram of Gamma ray detection system	5-3

5-3	Spectrum of Be^7 Gamma rays in NaI detector (upper and method of stripping background)	5-4
B-1	Geometry of scattering to produce recoil implantation	B-3
B-2	Cross section used for $p(\text{Li}^7, \text{Be}^7) n$ reaction	B-6
B-3	Differential cross section in lab coordinates for several energies	B-10
B-4	Graphical relationship between center-of-mass and laboratory velocities of recoil atoms. Note that 2 center-of-mass angles and 2 lab velocities are allowed for 1 lab angle	B-12

LIST OF TABLES

<u>Table</u>		<u>Page</u>
3-1	Planned wear test matrix for Phase II program	3-2
3-2	Scope of pin-on-disk test conditions	3-5
3-3	Selected test conditions	3-5
4-1	Nuclear Tagging Reactions	4-2
7-1	Exempt quantities of radioactive materials	7-1
7-2	Radiation dose rates and doses from common sources	7-2
A-1	Calculation of count rate in bearing test rig	A-3
A-2	Calculation of count rate in pin-on-disk test	A-4

SECTION 1

INTRODUCTION

Ceramic bearing technology is rapidly becoming a viable option in the design of high temperature gas turbines. However, much of the basic design data on the tribological properties of these materials is still lacking.

The objective of this program was to determine the feasibility of measuring some of the wear properties of ceramic bearing materials in real time without disturbing the wear couple or the operating conditions, such as temperature or break-in geometry.

The method chosen is to selectively introduce a radioactive tag into the surface of a ceramic part and to measure the wear amount by monitoring the strength of the tagging activity as the test progresses. Although this method, called Surface Layer Activation (SLA), has been used for many years in the automobile (1)(2) and heavy machinery industries (3)(4), it has not yet been used to measure the extremely minute amounts of wear which are experienced by ball bearings.

This program was analytical in nature, and its principal task was to show the feasibility and accuracy of such a technique applied to Si_3N_4 and SiC ceramic bearing components. In addition the goal was to develop the analytical theory, computer software and operational techniques needed for wear tests.

The primary findings of the program are:

1. The method for tagging Si_3N_4 , SiC , and M50 bearing components to depths of interest in bearings (1-20 microns) was developed, and subcontractors with the capability to implant these isotopes were identified.

2. Calculational techniques were developed to predict

activation and count rates in the detector system for both the pin-on-disk and bearing test rig.

3. The data acquisition electronics were selected and vendors identified.

4. Radiation Safety issues were examined and found to be not a problem. Activities required were below values exempt from regulation by the NRC or the States.

5. The use of the technique was proven feasible and valuable in measuring needed wear parameters in materials and conditions important to ceramic bearing operation.

SECTION 2

BACKGROUND

The ball and roller bearings used in gas turbines are generally made of steels (M50, 52100), and loss of bearing performance due to mild wear is not a normal failure mode. In liquid lubricated bearings, the lubricant serves to provide full separation of the rolling element and raceway which prevents wear. The lubricant also acts as a convective heat transfer medium to carry the heat out of the bearing and to equalize the temperature of the various components. Ceramic bearings, either non-lubricated or with solid lubricants, are unlikely to ever operate at full separation between the contact surfaces, and therefore mild wear is of concern. For example, Bunting⁽⁵⁾ has shown that a change in raceway conformity of an all ceramic bearing from 0.54 (as machined) to 0.505 due to mild wear can lead to thermal run away and bearing seizure. Thus the measurement of mild wear in a ceramic bearing is much more important and probably should be monitored in real time to prevent catastrophic failure in flight service.

In addition to this special vulnerability of ceramic bearings to mild wear, the tribological properties are not well understood and the amount of test data available is sparse compared to what is presently known about bearing steels. Clearly there is a need to accumulate basic tribological and bearing test rig data on the performance of ceramic bearing materials under various startup loads and lubrication schemes as well as various operating temperatures.

The SLA activation technique is capable of providing wear rate data in real time from initial break-in to final equilibrium without disassembling the wear couple. The proposed thin layer activation method was developed several years ago to make in-situ

measurements of the surface wear of parts in mechanical systems. It is particularly suited to the measurements of surface wear in areas which are generally inaccessible when real-time data are required, or where conditions make other physical measurement methods impossible. The original application of the technique, invented by the principle investigator while at McDonnell Douglas Corporation in 1971, was to measure the erosion of missile nosetips during atmospheric re-entry. The system required wear measurements to be made during the flight itself since no worn part could be recovered. The basic structure of the measurement system, as shown in Figure 2-1, consisted of two parts: an activated volume of the test component and a Sodium Iodide gamma-ray detector. The nosetip was first made radioactive by the bombardment of a proton beam which produced Be^7 from the carbon material. In flight, the detector measured the radiation being emitted by the activated material, which was a function of the thickness of material remaining. This radiation measurement, or count rate, was related to the exact eroded depth by a calibration curve obtained prior to the missile flight.

In applications involving mechanical systems, the concept is similar. The wearpoint of interest is either directly bombarded with a high energy beam of nuclei from a suitable atom accelerator, or radioactive atoms are embedded in the test sample as a secondary scattering process. The geometries involved will be shown in a later section, but in either case, the result is a shallow layer of lightly doped radioactive tracer atoms that can serve as an indicator of thickness removed. Figure 2-2 shows how the technique has been applied to real-time measurement of wear in a piston ring. Figure 2-3 shows how the gamma rays are detected outside of the automobile engine while it is running.

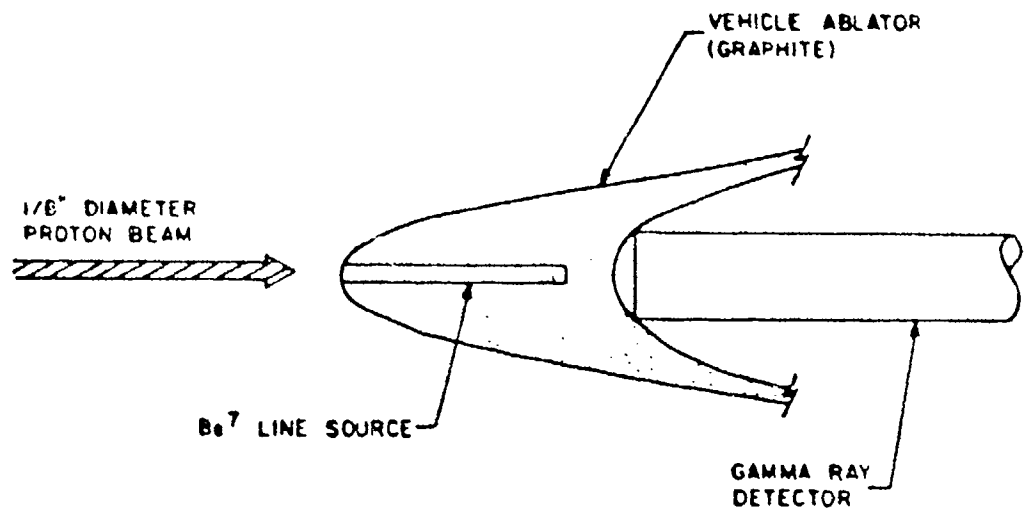


FIGURE 2-1. ORIGINAL APPLICATION OF THE SLA TECHNIQUE TO NOSETIP EROSION DURING RE-ENTRY.

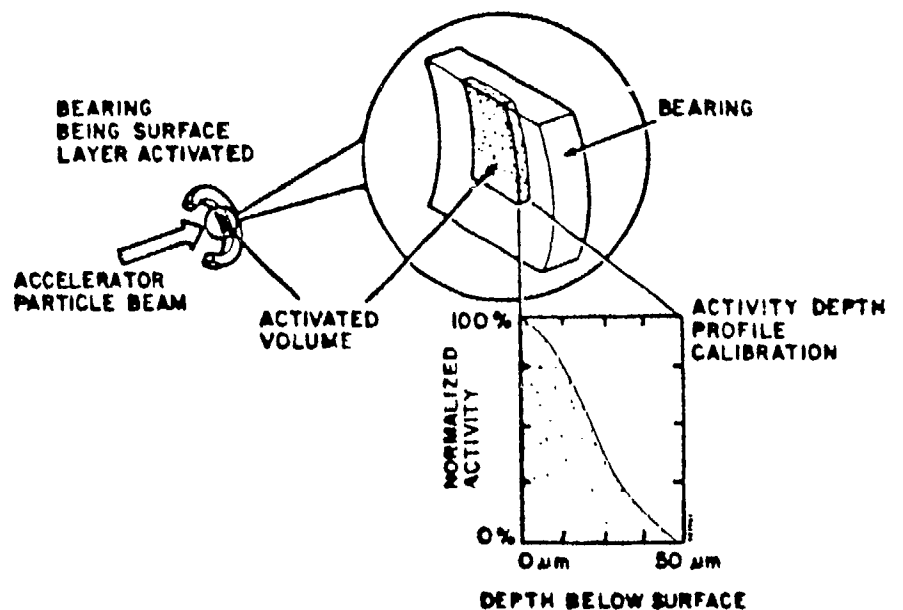


FIGURE 2.2. PISTON RING ACTIVATION OF A THIN SURFACE LAYER SHOWING THE ACTIVATION DEPTH PROFILE.

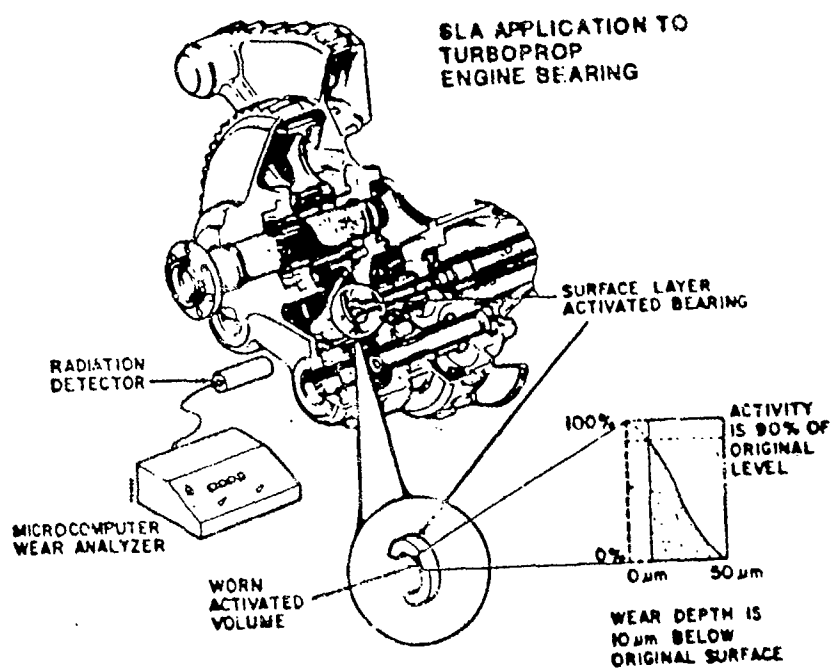


FIGURE 2-3. OUTSIDE RACE IN OPERATING POSITION BEING CONTINUOUSLY MONITORED BY A GAMMA RAY DETECTOR OUTSIDE OF A TURBOPROP ENGINE.

SECTION 3

SELECTION OF BEARING WEAR EXPERIMENTS

The experimental program will attempt to simulate wear on an all ceramic Si_3N_4 or SiC bearing as well as wear of the metal races in a hybrid bearing. In addition, two type of wear on the ceramic will be investigated. Wedeven⁽⁶⁾ at SKF has shown two distinct types of wear debris generated by Si_3N_4 rolling contact. At high contact stress with traction, Hertzian stress cracks form at the edges of the contact area and cause fracture. These conditions cause large particle spallation resulting in larger size particles ranging from 2 microns to 5 microns.

At lower loads, the surface becomes highly burnished and thin films of transparent wear debris of extremely small size are generated. This fine debris has been shown⁽⁷⁾ to be amorphous hydrated silicon oxide ($\text{SiO}/\text{XH}_2\text{O}$), which is softer than Si_3N_4 and may be a significant solid lubricant in high temperature dry operation.

The high contact stress wear can be measured using a pin-on-disk wear apparatus where the elements in the ceramic can be activated using the reaction:



in Silicon Nitride or



in Silicon Carbide

This will produce a surface layer about 10 to 50-microns deep which is doped with Be^7 , a gamma emitter with a 53 day half-life. At lower contact stresses a second type of activation can be used to produce an ultra-shallow, 1-micron (40-microinch) layer containing radioactive Be^7 . This type of activation can be used to detect the presence of the burnishing wear, which produces very fine SiO_x sheets about a few millionths of an inch thick.

Table 3-1 shows a summary of the types of test apparatus that might be used for the activation methods. The pin-on-disk apparatus is already in existence at Implant Sciences Corporation. The high load bearing test could be conducted using Government test facilities.

TABLE 3-1. PLANNED WEAR TEST MATRIX FOR PHASE II PROGRAM

TEST APPARATUS	LIGHT LOAD	HEAVY LOAD
pin-on-disk	Be^7 implant	Be^7 in Ceramic disk Direct Co^{56} in M50
High load Bearing Test rig	N/A	Be^7 in ceramic race Direct Co^{56} in M50

3.1 PIN-ON-DISK TEST

The pin-on-disk wear tester at Implant Sciences Corporation is shown in Figure 3-1. This tester has a contact force variable up to 10 GPa and can also measure sliding friction coefficients at velocities up to 40 cm/s.

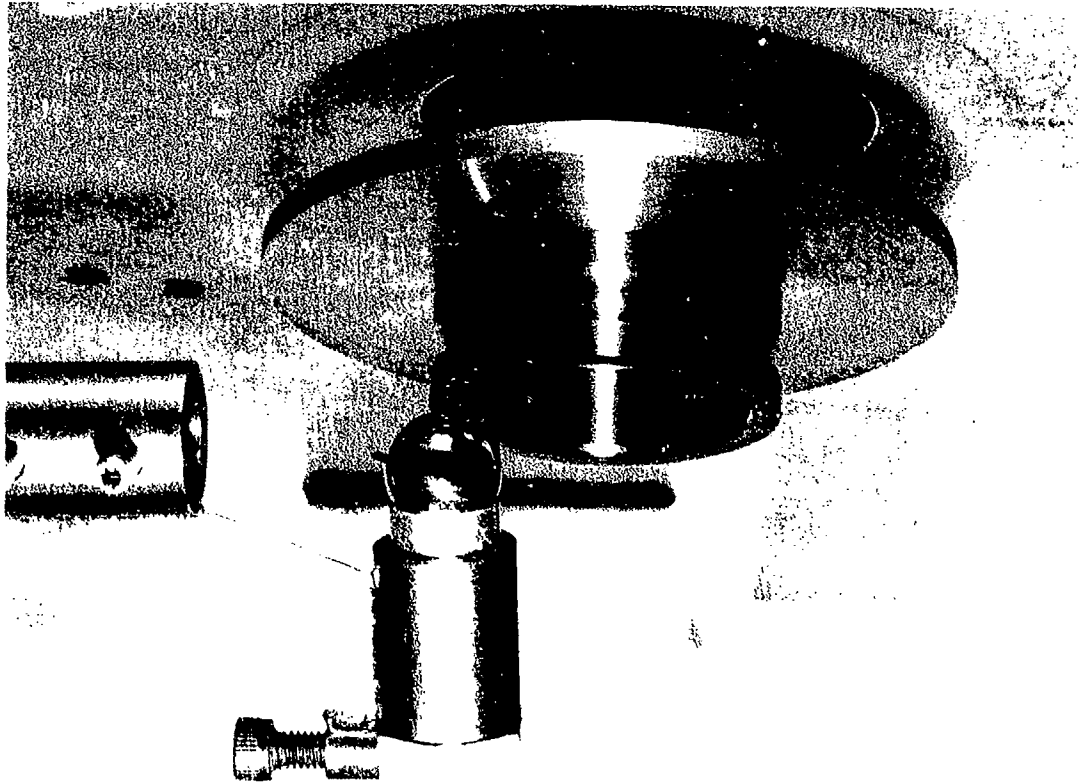


FIGURE 3-1. PHOTOGRAPH OF IMPLANT SCIENCES' PIN-ON-DISK TESTED WITH CERAMIC BALL ON M50 DISK.

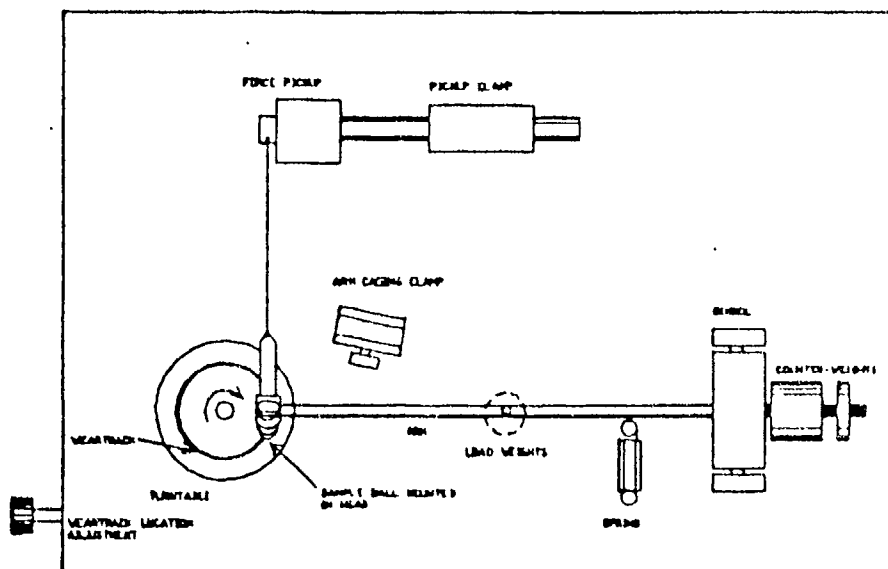


FIGURE 3-2. DIAGRAM OF IMPLANT SCIENCES' PIN-ON-DISK TESTER (TOP VIEW)

The tester can also be operated in a transparent glove box so that testing can be done in atmospheres other than air. Thermal insulation and a "clam shell" heater can also be added, so that the pin and disk can be raised to a temperature of up to 600°C. Figure 3-2 shows a plan-view diagram of the tester.

The pin-on-disk tests can be designed to simulate operational loads and sliding speeds. To this end we have selected the same silicon nitride bearing size and conditions described by Bunting (5) of SKF for our feasibility analysis. This paper describes a test of an all ceramic bearing with the following parameters:

OD of inner race	36 mm
Speed	38,000 r/min
Hertzian stress	2.07 GPa
Temperature	up to 600°C
Test duration	up to 246 minutes
Calculated sliding speed	1.32 m/s (1.8%)
Total race way wear	13 μ m (10 balls)

Since a pin-on-disk test is 100% sliding rather than 1.8%, the equivalent sliding distance turns out to be 1.95×10^4 meters which could be simulated in 28.7 hours at 100 r/min. Thus on Implant Science Corporation's pin-on-disk apparatus for Silicon Nitride using 2.07 GPa Hertzian stress and 100 r/min disk speed, a 28.7 h. run should yield about 1 micron of wear on the disk (at 600°C). This simulation and predicted wear depth will be used in the next section to determine the nuclear tagging method to be used.

Table 3-2 shows the total scope of all test conditions available with the present pin-on-disk apparatus. If one uses three values for each parameter, then the total number of tests could be 3^5 or 243. A more realistic test matrix has 12 tests and is shown in Table 3-3. These test conditions, a subset of Table

3-2, were selected to test the maximum capabilities of each of the three wear couples chosen. The final set of test conditions will be selected with consultation and approval of the AF project technical officer.

For each of these tests the disk wear as a function of time can be measured using the nuclear wear gauge. This can be done without stopping the rotation and therefore distributing the break-

TABLE 3-2. SCOPE OF PIN-ON-DISK TEST CONDITIONS

<u>Parameters</u>	<u>Test Conditions</u>
Hertz stress	0.2 —————> 2 GPa
Speed	10 —————> 100 r/min
Temperature	20°C —————> 600°C
Lubrication	none —————> powder
Wear couple	(1) ceramic pin/ceramic/disk (2) ceramic pin/M50 disk (3) M50 pin/ ceramic disk

TABLE 3-3. SELECTED TEST CONDITIONS

	Hertz Stress	Speed	Temp	Lube	Diskwear Expected
ceramic pin/ceramic disk	2 GPa	100	650° 20°	none powder	1 µm
ceramic pin/M50 disk	2	100	300°C 20°	none powder	10 µm
M50 pin/ceramic disk	2	100	300°C 20°	none powder	1 µm

in conditions. Data can be taken typically every hour except that during the initial start-up and break-in period data may be taken every 1 minute in order to determine break-in wear rates. Wear cannot be measured on the pins. In a pin-on-disk test, unlike a ball bearing, the same point on the pin is always in contact, a condition which can generate untypical wear rates and surface temperatures. The disk, on the other hand has a ring wear groove which has time to recover and cool during each revolution.

In addition to the nuclear wear measurement, the friction force and the temperature will be measured during each test.

3.1.1 PIN-ON-DISK TEST GEOMETRY

The Implant Science Corporation's pin-on-disk tester ordinarily uses a ball, typically 1/2 ins diameter as the pin and the flat side of a bearing ring as the disk. Because of the SLA technique, the ball geometry must be changed to a cylinder or a roller. The reason for this is illustrated in Figure 3-3.

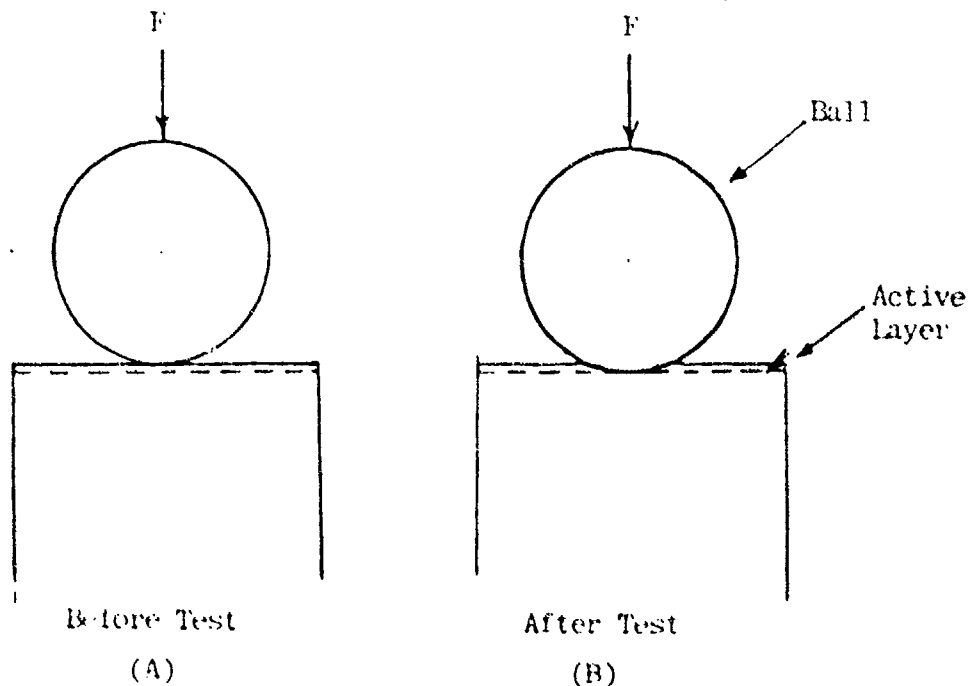


FIGURE 3-3. BALL BEARING ON FLAT DISK. LEFT SIDE BEFORE TEST, RIGHT SIDE AFTER WEAR GROOVE WORN.

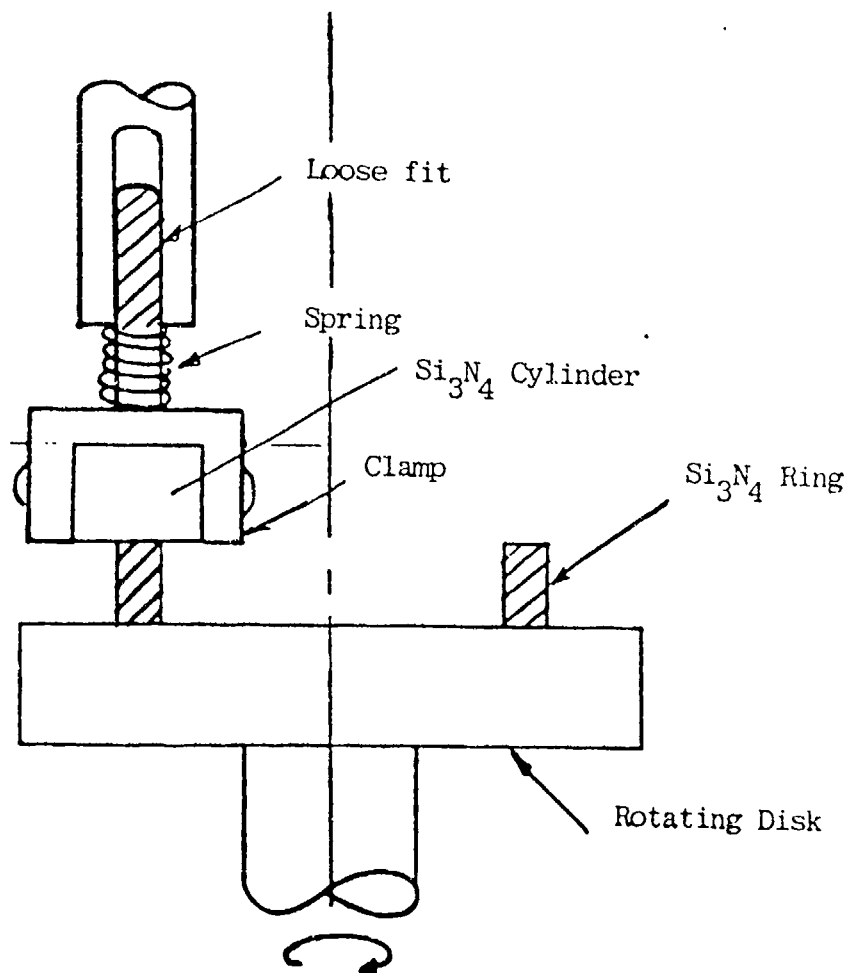


FIGURE 3-4. SCHEMATIC OF STATIONARY ROLLER (PIN) ON SLA ACTIVATED RING (DISK).

Before the test the activated surface is of uniform thickness, parallel to the ring edge. When the ball wears the disk (the ball wears too), the activity is not removed in level manner. The calibration procedure to be described in Section 6 requires the wear front to be perfectly parallel to the P surface. In order to wear the top of the ring and the pin in the same manner as the calibration procedure, it is necessary to use the side of a roller as the pin. This insures that the ring will not wear only in a narrow line where the ball touches it. Since it is critical that the roller is always seated parallel to the ring (the roller doesn't roll in this test, it only slides) it must be able to tilt from side to side to always rest parallel to the top surface of the ring. Figure 3-4 shows the method which can be used to achieve this.

The apparatus will also have a pair of clam-shell resistance heaters around the disk to heat the disk and roller up to 600°C. The gamma ray detector can view the ring from the side through the two Aluminum reflectors and thermal insulators. There should also be a vacuum pickup continuously sucking the wear debris away from the ring. The analysis of the count rates and accuracies of the measurement will be discussed in Section 4.

3.2 HIGH SPEED BEARING RIG TESTS

For this analysis we have tentatively selected an all ceramic roller bearing of approximately 30 mm bore and 62 mm O.D. for ease of activation. The inside race would be activated in a 1/8 in wide strip in the center of the O.D.

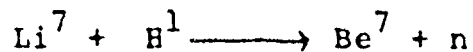
The narrow band of activity insures that the roller will wear the activity off uniformly, which is also the reason for selecting a roller rather than a ball bearing. At high speeds, a roller bearing operates close to a mode known as outer raceway control. This is caused by greater ball loading on the outer raceway due to centrifugal force, and it makes most of the slip or spin occur on the inner raceway, resulting in local heat and wear. For this reason we have selected the inner raceway as the nuclear tagged surface.

Following the analytical method of Bunting⁽⁵⁾ we project that about 13 to 15 microns of wear can occur before heat generation becomes intolerable. On this same size bearing, Bunting computes that the as-machined conformity of 0.54 becomes 0.505 with 13 micron of wear from the inner race. Figure 3-5 shows that thermal runaway is starting to occur at a conformity of 0.51.

In order to activate Silicon Nitride or Silicon Carbide to a depth of 2 to 13 microns, the recoil implant technique will be used. This method, which will be described in more detail later,

uses an auxillary nuclear reaction to generate high energy Be^7 , which is then implanted into the target.

The reaction is:



After the inner race is implanted, the actual test configuration will be similar to the bearing test rig shown in Figure 3-6.

Although this is not a schematic of an available test rig, it illustrates the shielding and detector distance involved in such a test. The gamma ray detector parameters for this candidate test are:

Detector distance= 8 in	Steel thickness=1/2 in
Detector Diameter= 6 in	Si_3N_4 thickness=3/4 in
Detector Eff= 0.8	

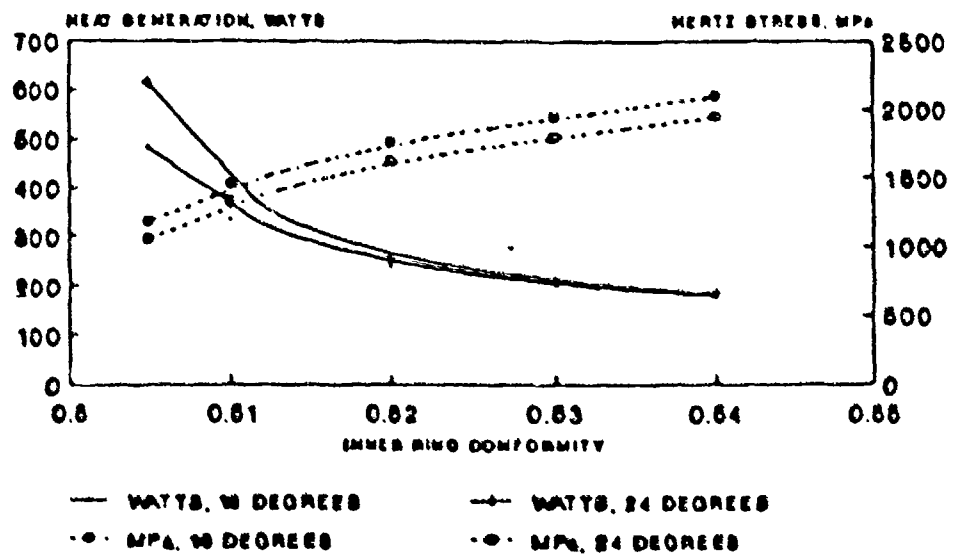


FIGURE 3-5. INNER RING HEAT GENERATION AND HERTZ STRESS AS A FUNCTION OF INNER RING CONFORMITY AND CONTACT ANGLE.

Using the computer program developed during this program, (see Appendix A) the total inner race activity for a count rate of 100 cps is 0.6 microcurie. This is a small amount of activity and should pose no great problem in performing such a test. It is in fact below the limit of regulation by the NRC. (See Section 8)

The detailed method of activation and calibration of this inner race will be covered in section 4 and 6.

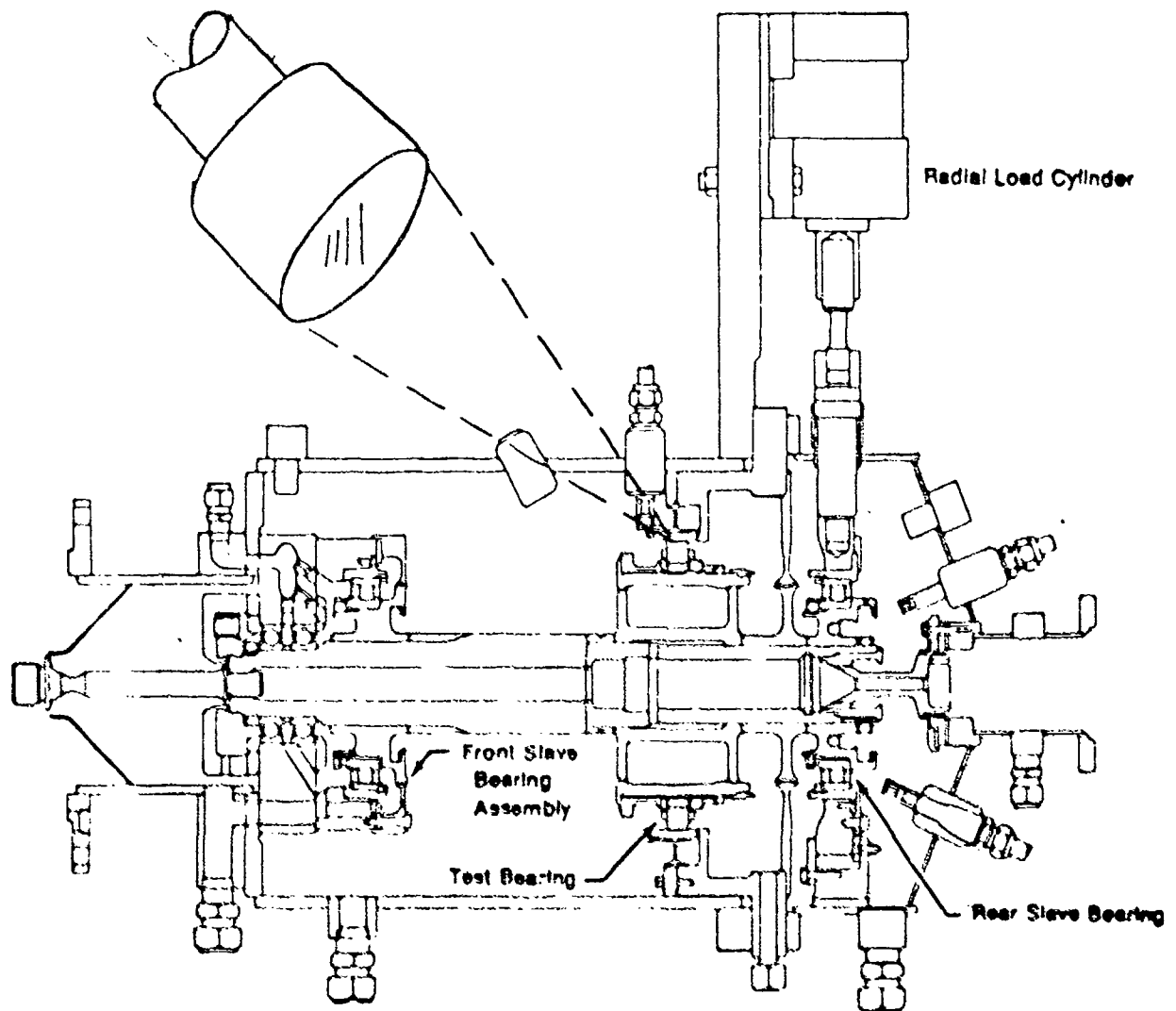


FIGURE 3-6. SCHEMATIC OF TYPICAL BEARING TEST RIG AND GAMMA RAY DETECTOR IN POSITION.

SECTION 4

DETERMINATION OF NUCLEAR TAGGING METHODS AND DETECTION

Measurements of surface material loss have been performed using a variety of nuclear activation techniques which differ mainly in the volume of sample material which is made radioactive.

The SLA technique differs from the older neutron activation method in that only the near surface zone of a part is activated. SLA activation is accomplished by using a directed beam of ions, which have only a very shallow depth of penetration into the part. Neutron activation is by total immersion in which the entire mass of the part is activated. The additional activated volume, essentially all of the sample, is not necessary for the measurement and only serves to increase background and impose serious safety problems.

A typical 3 in OD race will have a layer 10 microns thick by 1/8 in wide when activated using the SLA technique. The radioactivity in this volume is volume 0.5 microcurie and is quite satisfactory for an SLA measurement. An equivalent activation density and measurement sensitivity using thermal neutrons would require the total source strength to be approximately 2500 times greater, and this is a significant strength source.

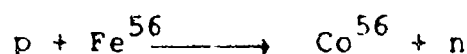
To achieve these extremely shallow implants of active material two methods are used:

- (1) Direct nuclear reaction in the part (useful from 1 to 1000 micron depths)
- (2) Implantation of active recoil atoms from an auxiliary reaction (useful 0.3 to 10 micron depths)

4.1 DIRECT NUCLEAR REACTION METHOD

In this method a nuclear reaction with a constituent atom in

the part is used to manufacture an active atom. For example, in steels, the iron atoms are reacted with an incoming beam of protons and some of them (a very small fraction) are transmuted to Co^{56} , which is unstable and emits gamma rays. The reaction can be written:



This requires a minimum of 10MeV protons for the reaction to occur. This reaction has been used by many workers to measure wear in steels. Similarly, Silicon Nitride or Silicon Carbide can be reacted with protons to form Be^7 or Na^{22} as desired. Part A in Table 4-1 shows the reactions of interest in this program for activating ceramic or steel bearing materials.

Table 4-1. Nuclear Tagging Reactions

(A) Direct Methods	Typical Depth Micron	Half- Life	Gamma Ray Energy	Activation Rate
$\text{C}^{12} (p, pn) \text{Be}^7$	10-500	53d	0.5MeV	med
$\text{N}^{14} (p, 2\text{He}^4) \text{Be}^7$	10-500	53d	0.5MeV	low
$\text{Si}^{28} (p, \text{Be}^7) \text{Na}^{22}$	5-100	2.7yr	1.27MeV	low
$\text{Fe}^{56} (p, n) \text{Co}^{56}$	10-30	77d	1MeV	high
<u>(B) Recoil Methods</u>				
$\text{H}^1 (\text{Li}^7, \text{Be}^7) n$	1-10	53d	0.5MeV	high
$\text{C}^{12} (\text{N}^{14}, \text{Na}^{22}) \text{He}^4$	0.5-5	2.7yr	1.27MeV	med
$\text{Fe}^{56} (\text{H}, \text{Co}^{56}) n$	0.3-1	77d	1MeV	low

For the pin-on-disk tests described in Section 3, a direct activation of the Nitrogen in Silicon Nitride was proposed to form Be^7 to a depth of 10 microns.

Figure 4-1 shows the geometry used for the calculation of count rate in the pin-on-disk test. The activity counted by the detector A, is given by

$$A = A_0 \Omega \epsilon e^{-\mu_p t}$$

where:

A_0 is the Be^7 activity induced in the disk

Ω is the solid angle to the detection

$e^{-\mu_p t}$ is the gamma ray attenuation through the shielding

ϵ is the detector efficiency for Be^7 gamma rays

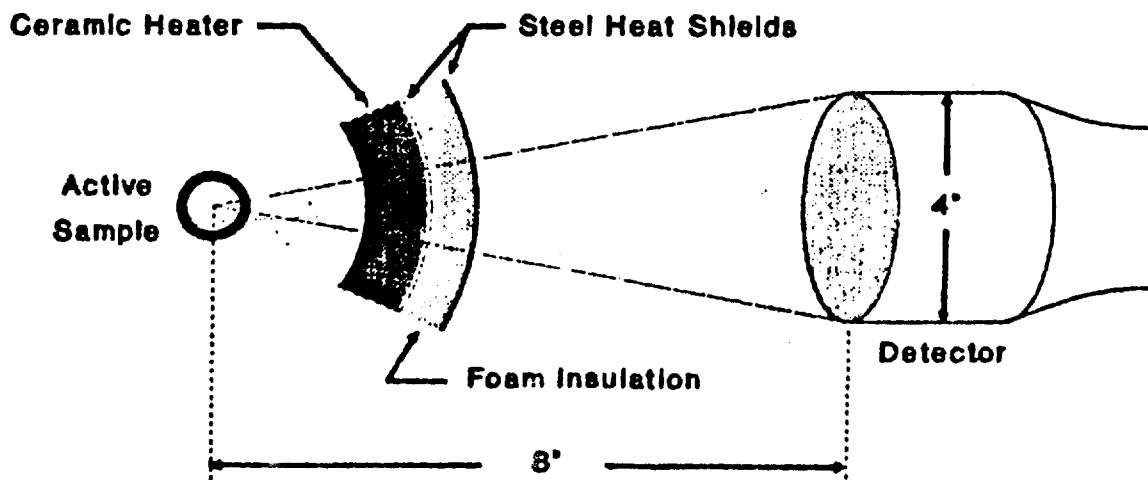


FIGURE 4-1. GEOMETRY FOR CALCULATION OF COUNT RATE IN PIN-ON-DISK

The details of this calculation and a computer program written to solve this equation can be found in Appendix A.

The results show that a Be^7 activity of only 0.5 microcuries can give a count rate of 300/s. This means that if a measurement is made for 1 minute per sample, there will be a statistical accuracy of 0.7%. The overall accuracy is also dependent upon the accuracy of the calibration curve, which will be discussed in Section 6.

4.2 THE RECOIL IMPLANTATION METHOD

In this method the nuclear reaction induced by the proton beam occurs in an auxiliary target, and the part in question "catches" the reaction products by being placed close to the target. The geometry is shown below in Figure 4-2.

This method was pioneered by T.W. Conlon at Harwell Laboratory (England). This method is particularly useful when the wear depth is very shallow (1-10 microns) or when the part cannot take the direct heat of the proton beam, such as for plastics or glass.

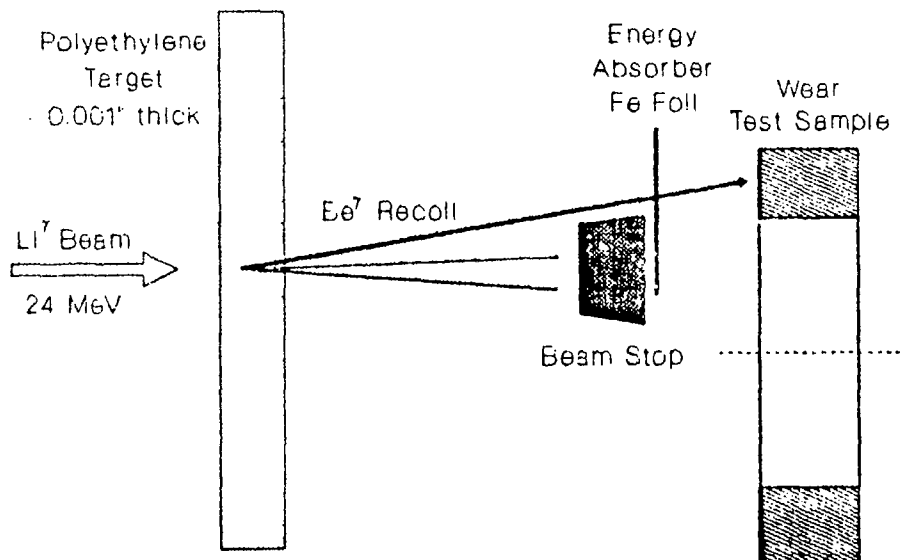
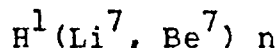


FIGURE 4-2 GEOMETRY USED DURING ACTIVATION BY RECOIL IMPLANTATION OF Be^7

The recoil reactions of interest for this program are shown in Table 4-1 part B. For the full-scale Silicon Nitride bearing tests described in Section 3.2, the reaction



has been chosen for quantitative analysis. In this case a polyethylene target is bombarded by a Li^7 beam from a tandem Van de Graaff accelerator. Using this reaction with 24 MeV Li^7 incident, the energy spectrum of Be^7 atoms impinging on the wear part prior to any energy attenuating foils is shown in Figure 4-3. The spectrum is input into Implant Sciences PROFILE CODE, and the calculated implanted depth profile of Be^7 atoms is shown in Figure 4-4. An energy absorbing foil convenient adjusts the Be^7 from the surface to a depth of 10 microns for a ceramic bearing test. The calibration curve would then have a resolution of about 0.05 micron per point. This resolution should be sufficient to measure wear rates during break-in as well as during equilibrium.

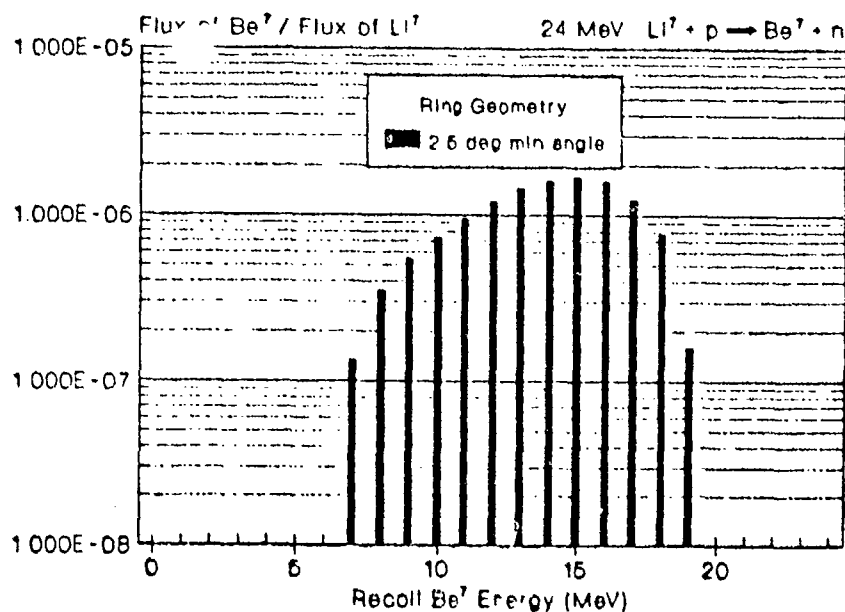


FIGURE 4-3. SPECTRUM OF Be^7 NUCLEAR GENERATED BY INELASTIC RECOIL REACTION.

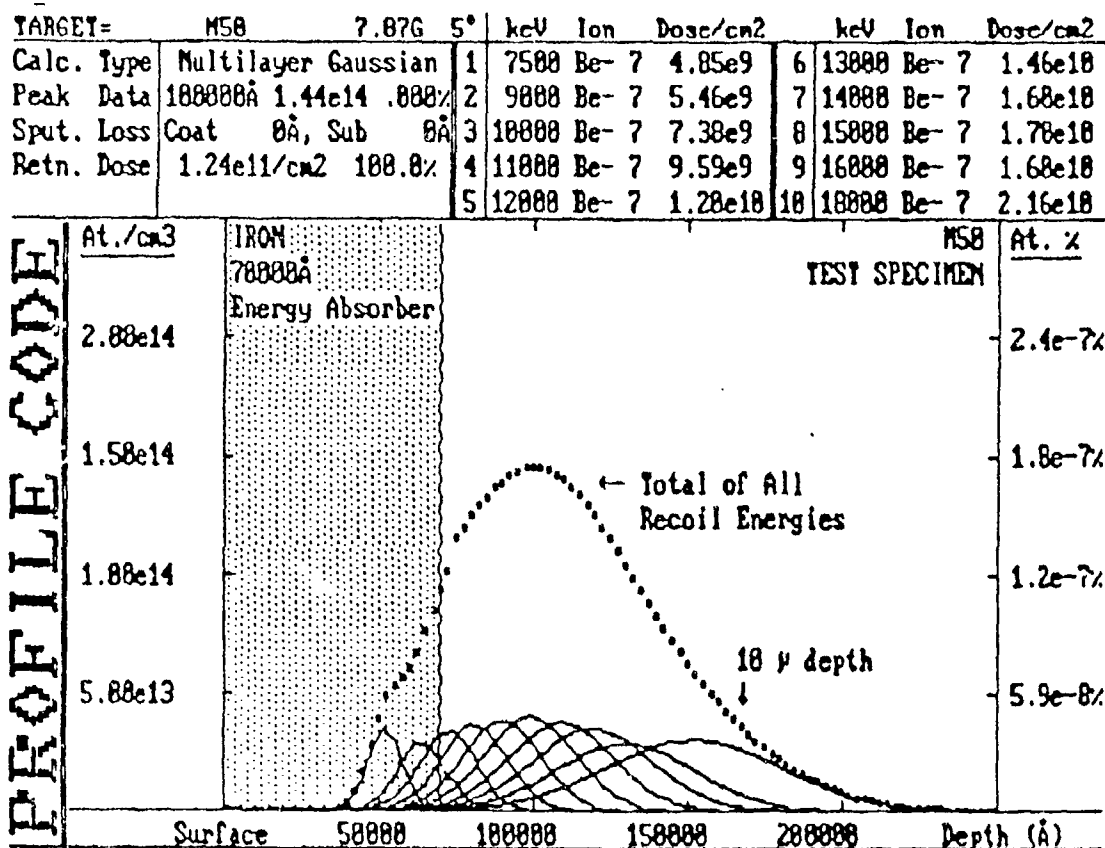


FIGURE 4-4. CALCULATION OF DEPTH PROFILE OF EACH ENERGY BIN OF Be^7 RECOILS IN M50

SECTION 5
DATA ACQUISITION SYSTEM

The data which need to be collected during an SLA wear test is simply the number of gamma rays per second emitted by the wearing part and to the initial value of this rate before wear. If one includes the half-life correction then:

$$f = \frac{A}{A_0 e^{-\lambda t}}$$

where: $\lambda = \frac{\log 2}{T_{1/2}} \text{ day}^{-1}$
 $t = \text{days}$
 $T_{1/2} = \text{half life (day)}$

If this measured value of the count rate is then used in conjunction with a previously measured calibration curve, the wear amount can be directly read from the curve.

For example, using the calibration curve of Figure 5-1, if we measure a value of $f=92\%$ after 3 days of running, then the wear amount, is 5 microns.

The measurement of this count rate is usually done with the most sensitive gamma ray detector available. In this case a 4 in. or 6 in. diameter Sodium Iodide (NaI) scintillation detector is the best choice.

In a properly designed SLA system, the NaI detector sensitivity can be so high and the source activity so low, that a routine Geiger counter survey will show no activity at all. This is important to appease fears of radiation, however unjustified, by the many persons involved in the operation of a bearing test rig or an aircraft test.

The lowest cost instrumentation is a personal computer which is outfitted with an analog-to-digital converter. This will provide a low cost system for future experiments and can also become the basis for a low cost production unit when the wear monitoring system is deployed in wide use.

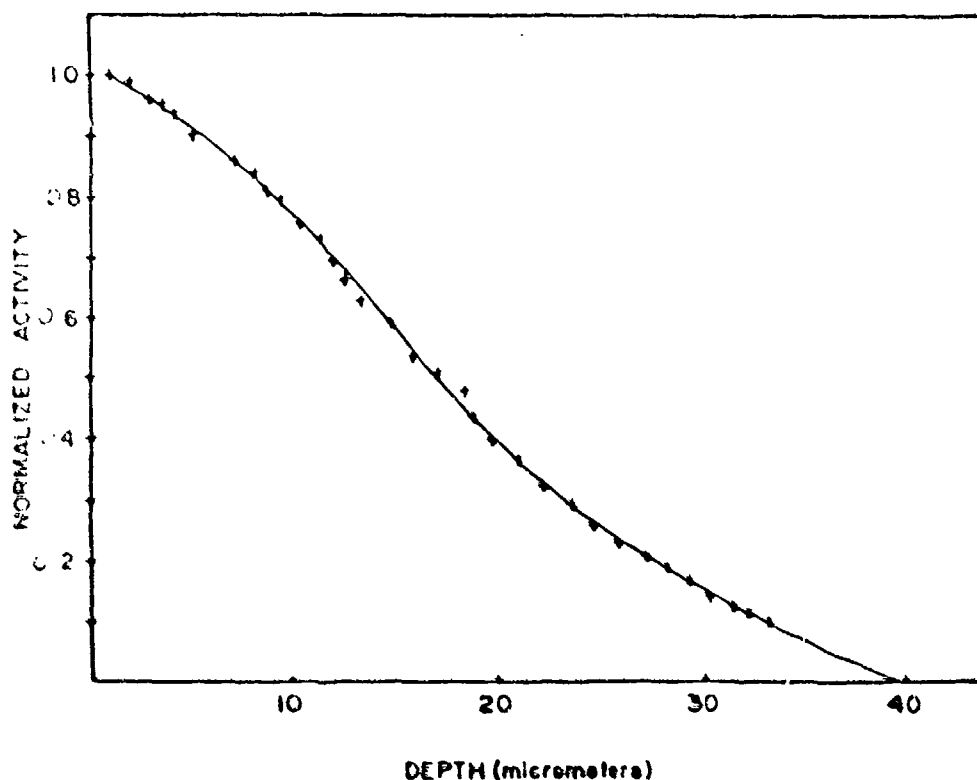


FIGURE 5-1. TYPICAL CALIBRATION CURVE IN SLA WEAR TEST.

The basic system design will include the components in the block diagram shown in Figure 5-2 below. All of the components are commercially available and therefore no engineering risk is involved in assembling such a system. The detector itself will be a 4" x 4" Sodium Iodine detector readily available commercially.

Once the gamma ray spectrum is in the computer, it will be stripped of background and fitted to a gaussian-shaped peak as shown in Figure 5-3. After fitting, the computer can also make the half-life correction, look-up the wear on the stored calibration curve, and display a plot of wear as a function test-time.

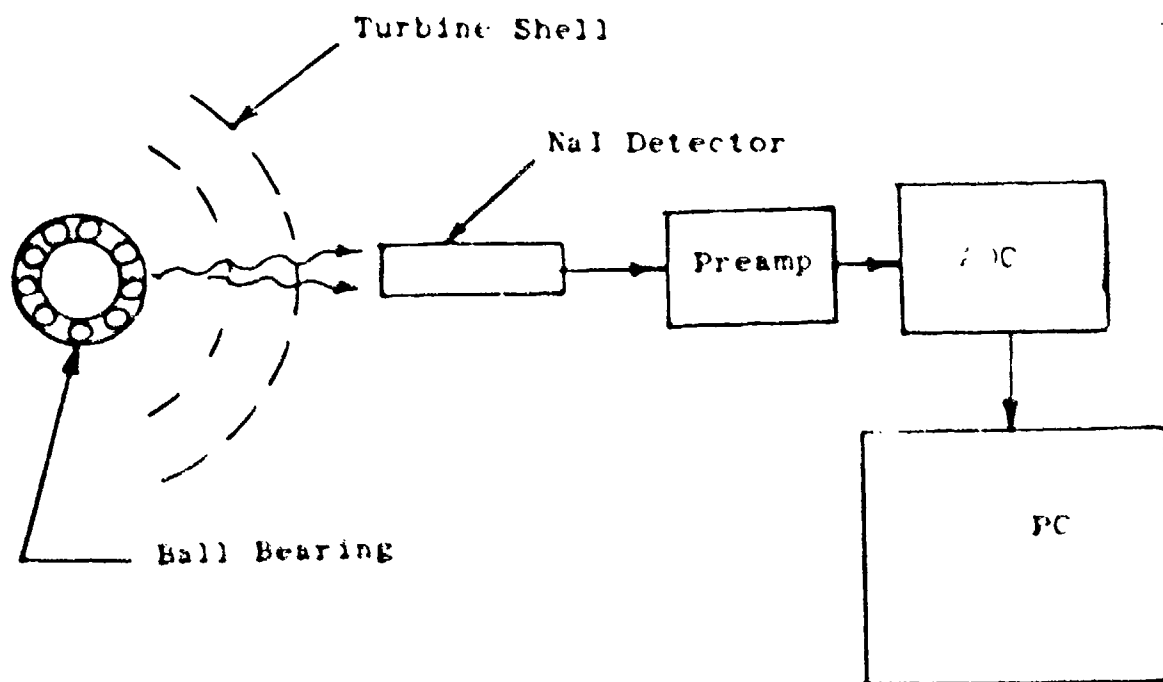


FIGURE 5-2 BLOCK DIAGRAM OF GAMMA RAY DETECTION SYSTEM.

The gamma detection system will be able to performance with both the pin-on-disk units and the bearing test rig with a total initial activity on the parts of less than 0.6 microcurie. This is below the limit of regulation by the NRC. (See Section 8)

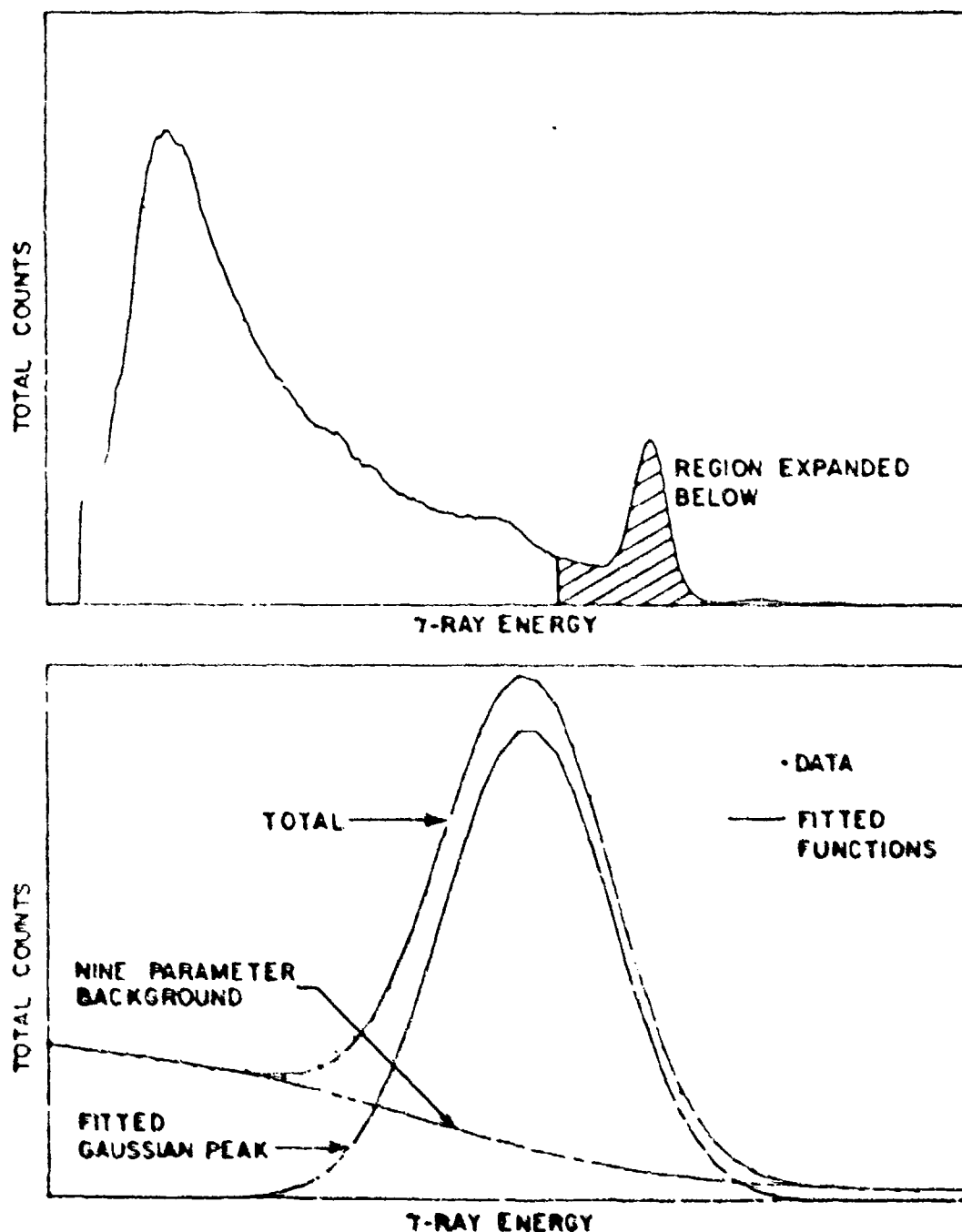


FIGURE 5-3. SPECTRUM OF Be^7 GAMMA RAYS IN NAI DETECTOR (UPPER) AND METHOD OF STRIPPING BACKGROUND

SECTION 6

CALIBRATION TECHNIQUES

In any SLA system, the accuracy of the measurement is limited by the calibration curve. This calibration curve is determined as follows:

1. Irradiate another piece of the wear component (the disk or the inside race) with the identical irradiation conditions and geometry as the prime part.
2. Artificially remove precise amounts of material. Measure the change in thickness with a precision micrometer and the change in activity content with the nuclear detection system.

This procedure yields a percent activity vs. depth curve such as previously shown in Figure 5-1. In most of the wear measurements of automobile piston rings and cams previously reported, the use of sandpaper was adequate since the activation depth was 30 to 1000 microns and measurement of changes in thickness were several microns (2.5 micron=0.1 mils) for each point on the calibration curve.

In the case of ceramic ball or roller bearings, where the expected wear is only a few microns, sandpaper cannot be used to "wear" away precise amounts on the calibration sample. At Implant Sciences we have developed a method of ion beam milling which can remove precisely known parallel layers of ceramics for calibration purposes.

An experiment was done during this program to measure the milling rate of high energy Xenon ions sputter eroding a Silicon Carbide specimen. We found that 36mA-h of 100keV Xenon directed on a flat surface of SiC milled away precisely 5.0 microns of material. The final measurement of 5.0 microns was done using a thin film profiler with a 0.05 micron accuracy.

Thus, by ion beam milling for 5% of the time (1.8mA-h), we can remove 0.25 microns and sequentially measure the loss of activity. Using this method a calibration curve of count rate observed vs. wear depth (in 1/4-micron increments) can be determined.

The problem of creating an accurate calibration curve is a critical issue in measuring very low levels of wear in bearings. It is believed that no other workers in the world have developed such a precision method using ion milling, and its use in this application could mean the difference between reliable data and uncertain results.

SECTION 7

RADIATION SAFETY CONSIDERATIONS

The radiation levels associated with the SLA technique are extremely low and are not subject to NRC regulation, because the levels are below the exempt quantities for the isotopes of interest. Table 7-1 shows that both Be^7 + Co^{56} needed for this program are below the exempt quantities in NRS regulation, paragraph 30.71. Also the dose rate from these active bearings should be about 0.1 mrem/h on contact and less than 0.02 mrem/h at 6 in. away. When shielded by the pin-on-disk apparatus or the bearing test rig, there should be no measurable radiation using a geiger counter. Ambient background is in the range of 0.01 to 0.02 mrem/h.

TABLE 7-1. EXEMPT QUANTITIES OF RADIOACTIVE MATERIALS

	Schedule B ⁽¹⁾ (μCi)	Need Radioactivity at start of test (μCi)
Be^7	1	0.6
Co^{56}	1	0.5
(1) NRC regulation (30.71)		

Table 7-2 shows how these levels compare to doses from common sources.

The only NRC regulation mandated during the installation and running of the test program is that a "Caution Radioactive Material" tag must be affixed to the box containing the parts. Also the radiation safety procedures required to assemble the

bearings unto the test rig are minimal or none. The only requirement is that the technician must be made aware that the parts are radioactive, but no special precautions are required.

TABLE 7-2. RADIATION DOSE RATES AND DOSES FROM COMMON SOURCES

	Dose	
	(mrem/h)	mrem
Potassium-40 naturally occurring in the body ^{*(1)}	0.002	20/year
Natural background dose at sea level (average) ⁽¹⁾	0.011	100/year
3-h jet-plane flight ⁽¹⁾	0.67	2/flight
Chest X-ray Source	-	30/exposure
Dental X-ray single exposure ⁽²⁾	-	250-450/exposure

(1) Reference 16

(2) Reference 17

*0.0118 percent of all potassium is potassium-40

SECTION 8

CONCLUSION AND RECOMMENDATIONS

This program investigated the technical feasibility of using the surface layer activation technique for the measurement of wear rates applicable to all ceramic and hybrid-ceramic ball bearings.

The general technique had to be modified to accommodate the extremely fine wear amounts experienced by ceramic bearings. An important aspect of the work was shown to be adjusting the depth penetration of the implanted isotope (Be^7) in the thinnest possible layer so that the maximum measurement sensitivity could be obtained. Another important issue that was successfully resolved was the calibration technique that had to be developed to measure wear differences with an accuracy at the 1/4-micron level. Specifically the conclusions reached during this work are:

1. The SLA technique, using Be^7 recoil implantation as the nuclear tagging isotope, is a particularly sensitive method of measuring wear in ceramic or metal rolling element bearings in-situ and with 1/4-micron resolution.
2. Techniques and software have been developed to calculate the precise isotope implantation concentrations and depths to yield a specific measurement accuracy and wear depth resolution.
3. Specific instrumentation and vendors have been identified to purchase and assemble a system for detection of the radiation signal. Also specific accelerator laboratories have been identified to perform the activation service for subsequent programs.
4. All of the necessary scientific and engineering issues have been resolved in preparation for implementation of this measurement both in the laboratory and in a bearing test rig of the Air Force's choice.

As a result of these findings, it is recommended that a follow-on program be initiated to move this technology from

the analysis phase into the laboratory. The test program should have the following specific components:

1. Pin-on-disk measurements of ceramic wear in various load, temperatures and lubrication conditions should be made. These measurements should include various ceramic-on-ceramic and ceramic on bearing steel wear couples.

2. The activation techniques necessary to perform should be implemented at an appropriate accelerator laboratory, and the samples should be used to verify the software predictions made in this study.

3. A calibration apparatus should be set up and wear calibration curves should be measured for several ceramic materials of interest.

4. A specific bearing should be selected for testing in a bearing test rig designated by the Government.

5. The wear test data received from the bearing test rig should be correlated to the basic pin-on-disk data generated at the beginning of the program.

REFERENCES

1. "Selective Radioactive Tracers for Engine Wear Diagnosis and Filter Avaluation." G.W. Jones, A.J. Armini, N.C. Schoen, Technical paper 780972, SAE meeting, Toronto, 1978
2. "The Use of Surface Layer Activation Wear Monitoring for Filter Design and Evaluation." F.L. Milder, A.J. Armini, Technical paper #810329, SAE International Congress, Detroit, Feb. 1981
3. "Thin Layer Activation by Accelerated Ions--Application to Measurement of Industrial Wear." T.W. Conlon, Wear, 29 (69-80) 1974
4. "The Method of Thin Layer Activation in Industry" Postnikov V.I., Moscow Atomizdat 1975
5. "Wear in Dry-Lubricated Silicon Nitride, Angular Contact Ball Bearings." B.G. Bunting. Technical paper STLE Annual Meeting, 1989
6. "Tribological Examination of Unlubricated and Graphite Lubricated Silicon Nitride Under Traction Stress." L.D. Wedeven, A. Pallini, N.C. Miller, ASME Wear of Materials 1987, Vol. 1, P. 333-347.
7. "Adhesion, Friction and Micromechanical Properties of Ceramics." K. Miyoshi, Surface and Coatings Technology 36 (1988)
8. Joseph F. Janni, Technical Report AFWL-TR-65-150, Air Force Weapon Laboratory, Air Force Systems Command, Kirland Air Force Base, New Mexico, 1966.
9. Claude Finley Williamson et al., Report CEA-R 3042, Department De Physique Nucleaire, Service de Physique Nucleaire a Basse Energie, La Documentation Francaise, Secretariat General Du Government, Direction De La Documentation, 16, Rue Lord Byron,

Paris, VIII^{eme}.

10. J. Ziegler et al., The Stopping and Range of Ions in Matter, Peranon Press, New York, 1985.
11. J. Ziegler, IBM Corp. Private Communication.
12. Robert A. Howard, Nuclear Physics, Wadworth Publishing Co., Belmont, Calif., Chapter 10.
13. John David Jackson, Classical Electrodynamics, John Wiley & Sons, New York, Chapter 12.
14. Harold Enge, Introduction to Nuclear Physics, Addison-Wesley, Reading, Mass., Chapter 13.
15. T.W. Conlon, AERE-R 9340, United Kingdom Atomic Energy Authority Harwell Report, 1979.
16. Wilson R. et al., "Energy, Ecology, and Environment," Academic Press p. 244 (1974).
17. Dental Exposure Normalizing Technique, U.S. Department of Health Education, and Welfare, Bureau of Radiological Health, Rockville, MO.

Appendix A

Calculation of Expected Count Rates in Detector

The calculation of gamma count rate in a Sodium Iodide detector is straightforward although there are numerous terms in the expression. Since many hundreds of calculations had to be performed in this program to select all of the free parameters, we decided to write a computer program to solve this problem.

In general, the expression for the count rate measured by a detector is

$$A = A_0 \Omega \epsilon \sum_1^n e^{-\mu_n \rho_n t_n} \quad (1)$$

where:

A_0 is the source activity in disintegrations/second

Ω is the solid angle fraction of 4-pi steradians

ϵ is the detector efficiency of the gamma ray of interest.

$e^{-\mu_n \rho_n t_n}$ is the attenuation coefficient of the n^{th} absorber.

The source in this case is either created by direct activation or by recoil implantation. Recoil implantation of Be^7 is discussed in Appendix B. Direct activation of Carbon, or Nitrogen in SiC , or Si_3N_4 , respectively, to form Be^7 in the surface is calculated using the following expression

$$A_0 = \lambda \left(\frac{N_A \rho}{M} \right) \frac{t}{8} \times 10^{-27} \int_0^{x_0} \sigma(x) I(x) dx \quad (2)$$

where:

λ = the radioactive decay constant

N_A = Avogadro's Number

ρ = density of target
 M = Atomic weight of target
 t = Activation time (in seconds)
 e = electronic charge
 $\sigma(\lambda)$ = reaction cross section (mb)
 $I(x)$ = Beam current (uA)
 activation depth = $R(E_0) - R(E_T) = X_0$

The result of two calculations, one for the pin-on-disk case, and one for the bearing test rig case are shown in Tables A-1 and A-2 respectively.

TABLE A-1
CALCULATION OF COUNT RATE IN BEARING TEST RIG
(RECOIL ACTIVATION METHOD)

DETECTOR	ABSORBERS	NUCLEAR REACTION
Distance = 8 inch	Steel = .5 inch	Sigma = 25 mbarn
Diameter = 6 inch	Si3N4 = .75 inch	Depth = 9.999999 micron
Efficiency = .9	Ceramic = 0 inch	Beam Current = 10uamp

Activity(Microcurie)	Beam Time(Minutes)	Count Rate(cps)
0.031	10.53	15
0.063	21.06	30
0.094	31.59	45
0.126	42.12	60
0.157	52.65	75
0.189	63.18	90
0.220	73.70	105
0.252	84.23	120
0.283	94.76	135
0.315	105.29	150
0.346	115.82	165
0.377	126.35	180
0.409	136.88	195
0.440	147.41	210
0.472	157.94	225
0.503	168.47	240
0.535	179.00	255
0.566	189.53	270
0.598	200.06	285
0.629	210.59	300

TABLE A-2

CALCULATION OF COUNT RATE IN PIN-ON-DISK TEST
(DIRECT ACTIVATION METHOD)

DETECTOR	ABSORBERS	NUCLEAR REACTION
Distance - 8 inch	Steel = .062 inch	Sigma = 25 mbarn
Diameter = 4 inch	Si3N4 = 0 inch	Depth = 9.999999 micron
Efficiency = .9	Ceramic = .25 inch	Beam Current = 10amp

Activity(Microcurie)	Beam Time(Minutes)	Count Rate(cps)
0.026	8.54	15
0.051	17.07	30
0.077	25.61	45
0.102	34.14	60
0.128	42.68	75
0.153	51.22	90
0.179	59.75	105
0.204	68.29	120
0.230	76.82	135
0.255	85.36	150
0.281	93.90	165
0.306	102.43	180
0.332	110.97	195
0.357	119.50	210
0.383	128.04	225
0.408	136.58	240
0.434	145.11	255
0.459	153.65	270
0.485	162.18	285
0.510	170.72	300

Appendix B

Calculation of Recoil Implanted Activity Versus Depth

The calculation of the quantity of radioactive recoil atoms deposited in a catcher sample is extremely complex. It is necessary to follow the reacting particles through each of the interactions and sum the contributions. The problem is made more difficult by the multi-valued nature of recoil energy versus angle and the fact that for thick targets, the nuclear reaction can occur for a variety of incoming beam energies. In the following, target refers to the sample struck by incoming beam, and catcher sample refers to the secondary target which receives recoils. The complete set of calculation steps based on the geometry of Figure B-1 is as follows.

1. Select initial starting parameters:
 - (a) incoming beam energy
 - (b) angle of incidence
 - (c) reaction of interest
2. Iterate on depth-below-surface where reaction takes place.
3. Calculate energy of incoming beam at point of reaction.
4. Determine angle from point of reaction to point in catcher sample.
5. Calculate both energies of recoil atom at this angle and beam energy.
6. Calculate differential cross section at this angle and beam energy.
7. Calculate energy loss through first target before escape to reach catcher sample (both scattered energies).

8. Calculate flux of recoils at the two energies incident on the catcher sample.
9. Calculate depth distributions of recoil atoms in catcher sample for both energies after correcting for energy loss in pre-absorber foil.
10. Repeat items 2-9 for all combinations of reaction location and angle which can occur. Because of cusps in the cross sections at the critical angles, fine steps are required.

This is not a straight forward calculation. Using simplified analytic functions for ion range versus energy, it still requires about 1 1/2 hours of computer time using a 20 MHz, 32-bit personal computer with math coprocessor. Older personal computers would need up to 15 hours to complete the problem.

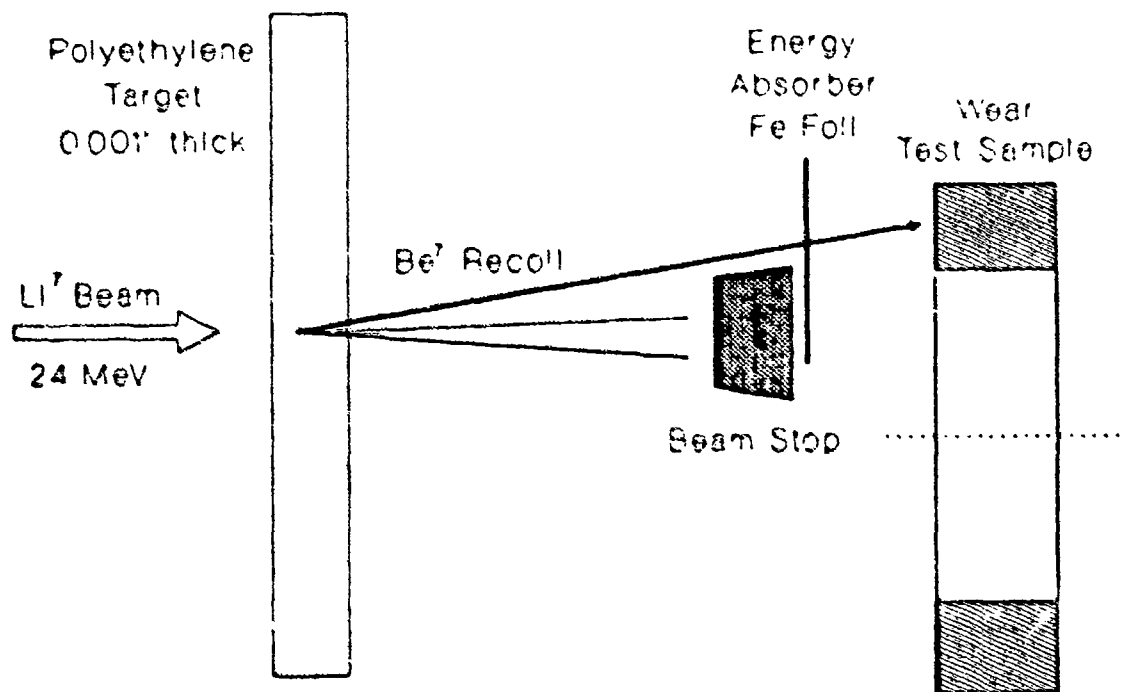


Figure B-1. Geometry of Scattering to Produce Recoil Implantation

Details of the more obscure mathematics involved will now be documented for the interested reader. References are provided for many of the equations used, and no effort is made to show intermediate calculations.

A. Range versus Energy

Computer programs exist to predict the mean range to stop an ion of a given energy in a given target. For light ions, such as protons, deuterons, or alphas, the fastest calculation method is to perform a mathematical fit to data from published tables (6,7). In general it is found that a plot of the log of range versus the log of energy is nearly a straight-line or a (quadratic) over a narrow enough energy band. Thus, one can write

$$\log R = A \log E + B \quad (3)$$

R = range E = energy

A, B = constants to be determined

This reduces the problem to a simple case of least squares fitting to tabular data to find A and B. Once obtained, one can use the convenient procedure of determining energy versus thickness traversed by the method of range differences. This is performed as follows:

1. Determine range R_{in} at incoming energy E_{in} using equation 1.
2. Subtract the thickness of material traversed, dx_{in}

$$R_{out} = R_{in} - dx_{in} \quad (4)$$

3. Substitute R_{out} back into equation 1 and solve for E_{out}

$$\log E_{out} = (\log R_{out} - B)/A \quad (5)$$

This method has the advantage of being fast to calculate although the span of energies accommodated with accuracy is limited. Tabular data for heavy ions has been taken from Implant Science Corporations' Profile Code, which uses a range program by Ziegler ⁽⁸⁾ with empirical modifications to match ranges calculated by Monte Carlo simulators, such as TRIM. ⁽⁹⁾

B. Scattered Flux

The ratio of incoming beam flux versus outgoing recoil flux from a reaction site is given by

$$\frac{\text{flux out}}{\text{flux in}} = \frac{d\sigma}{d\Omega} \frac{d\theta}{4\pi} \frac{d\phi}{M_0} \rho dt N_{AV} \quad (6)$$

$\frac{d\sigma}{d\Omega}$ = differential cross section in lab coordinates at angle and energy E

$d\theta, d\phi$ = angular spread on catcher sample for solid angle

ρ, M_0 = target density, mass

dt = increment of target thickness

N_{AV} = Avogadro's number, 6.023×10^{23}

This equation can be broken into the following components. The differential cross section is the probability of the reaction scattering a recoil into a unit solid angle at some angle. The angle variables give the actual solid angle. The remaining terms are the number of target nuclei that can participate in making a reaction.

C. Differential cross section.

Usually the differential cross section is not published as a function of many energies, although the total cross section is often available. The most difficult part of the overall calculation is this conversion between total and differential cross section. The total cross section of the reaction is shown in Figure B-2.

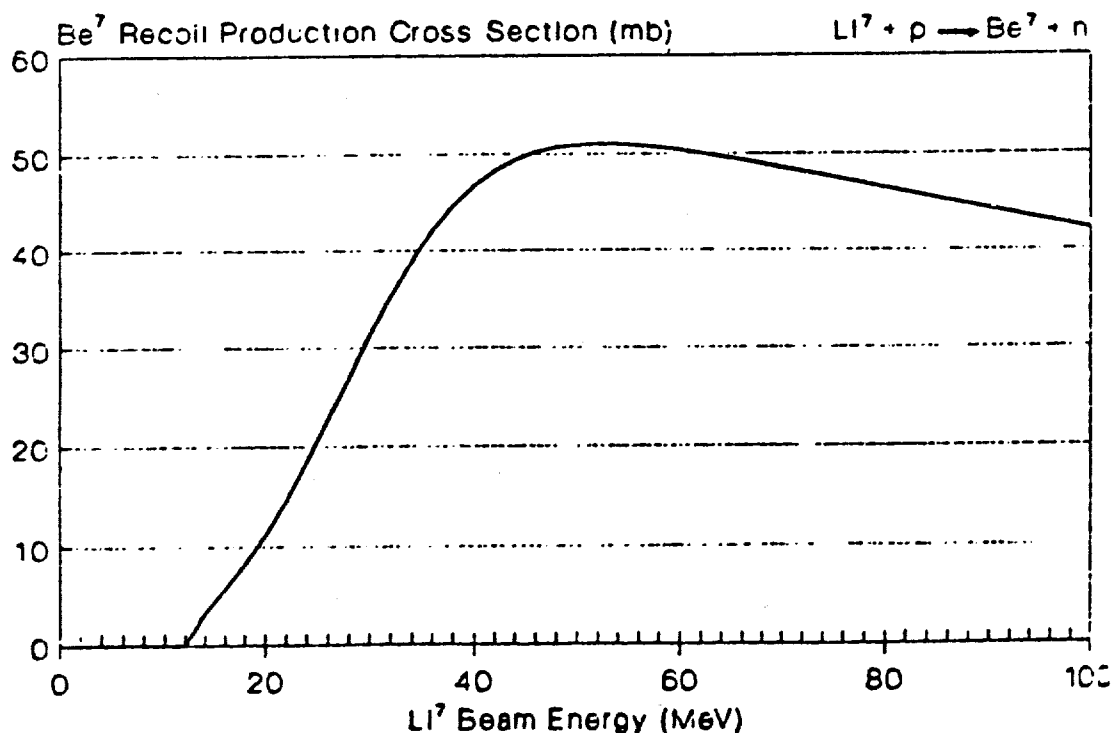


Figure B-2. Cross Section Used for $p(\text{Li}^7, \text{Be}^7)n$ Reaction

Many nuclear reactions are of the type known as compound nuclear reactions. In this model the incoming beam particle merges into the struck nucleus and mixes its energy in completely. Eventually, (after 10^{-20} seconds), recoil product atoms escape. Because of the mixing, information on the direction of the original incoming atom is lost, so the exiting recoil atoms "boil off" in arbitrary directions in the center-of-mass coordinate system. Thus, the differential cross section in the center-of-mass is a constant versus angle. The problem, then, is to convert a constant center-of-mass cross section to laboratory coordinates, integrate the resulting angular distribution, and normalize it to the total cross section as a function of energy. The procedure is a bit tedious.

The necessary equations are listed below. The entire calculation is relativistically correct. A prime indicates center-of-mass variable. (10,11,12)

$$\frac{\left(\frac{d\sigma}{d\Omega}\right)'}{\left(\frac{d\sigma}{d\Omega}\right)_{LAB}} = \frac{b_f^2 c^2}{\beta_B^2 c^2} \sqrt{1 - \frac{(W_B'^2 - b_f^2 c^2) \beta^{-2}}{b_f^2 c^2 (1 - \beta^2)} \sin^2 \theta_{LAB}} \quad (7)$$

θ_{LAB} = lab scattering angle of recoil particle B

$$b_f^2 c^2 = \frac{[Q(a+A+b+B)c^2 + 2W_{K1}Ac^2][Q(a+A+b+E)c^2 + 2W_{K1}Ac^2 + 4Bbc^2]}{4[2W_{K1}Ac^2 + (a+A)^2c^2]} \quad (8)$$

a, A, b, B are the masses, a is incoming, A is struck, B is the recoil of interest

W_{KI} = Kinetic Energy of a

$$Q = (a + A + b + B)c^2 \quad (9)$$

$$\bar{\beta}^2 = \frac{W_{KI}(W_{KI} + 2ac^2)}{[W_{KI} + (a + A)c^2]^2} \quad (10)$$

$$W'_B = \frac{E'^2 + (Bc^2)^2 - (bc^2)^2}{2E'} \quad (11)$$

$$E' = \sqrt{(ac^2)^2 + (Ac^2)^2 + 2E_1Ac^2} \quad (12)$$

$$E_1^2 = (W_{KI} + ac^2)^2 \quad \rho_1^2 c^2 = (W_{KI} + ac^2)^2 - a^2 c^4 \quad (13)$$

$$\rho_B^2 c^2 = E_B^2 - B^2 c^4 \quad (14)$$

$$E_B = (A_1 \pm A_2 A_3) / A_4 \quad \text{both signs physical} \quad (15)$$

$$A_1 = [E_1 + Ac^2][E_1 Ac^2 + \frac{1}{2}(a^2 + A^2 + B^2 - b^2)c^4] \quad (16)$$

$$A_2 = \sqrt{\rho_1^2 c^2} \cos \theta_{LAB} \quad (17)$$

$$A_3 = \sqrt{[E_1 Ac^2 + \frac{1}{2}(a^2 + A^2 - b^2 - B^2)c^4]^2 - b^2 B^2 c^4 - \rho_1^2 c^2 B^2 c^4 \sin^2 \theta_{LAB}} \quad (18)$$

$$A_4 = (E_1 + Ac^2)^2 - p_1^2 c^2 \cos^2 \theta_{LAB} \quad (19)$$

For normalization we have $\sigma_T(E)$ as experimental data and

$$\sigma_T(E) = C \int_0^{\theta_{CRIT}} \frac{d\sigma}{d\Omega_{LAB}} 2\pi \sin \theta_{LAB} d\theta_{LAB} \quad (20)$$

where θ_{CRIT} is determined from

$$\sin \theta_{CRIT} = \sqrt{\frac{Ab}{aB} \left(1 + \frac{Q}{W_{CM}}\right)} \quad (21)$$

$$W_{CM} = \frac{AW_{K1}}{(a+A)} \quad (22)$$

Equation 7 is summed over as many angles as practical in order to obtain C and get

$$\frac{d\sigma}{d\Omega_{LAB}} = C \frac{d\sigma}{d\Omega_{LAB}} \quad (23)$$

The final differential cross section vs. scattering angle is shown in Figure B-3.

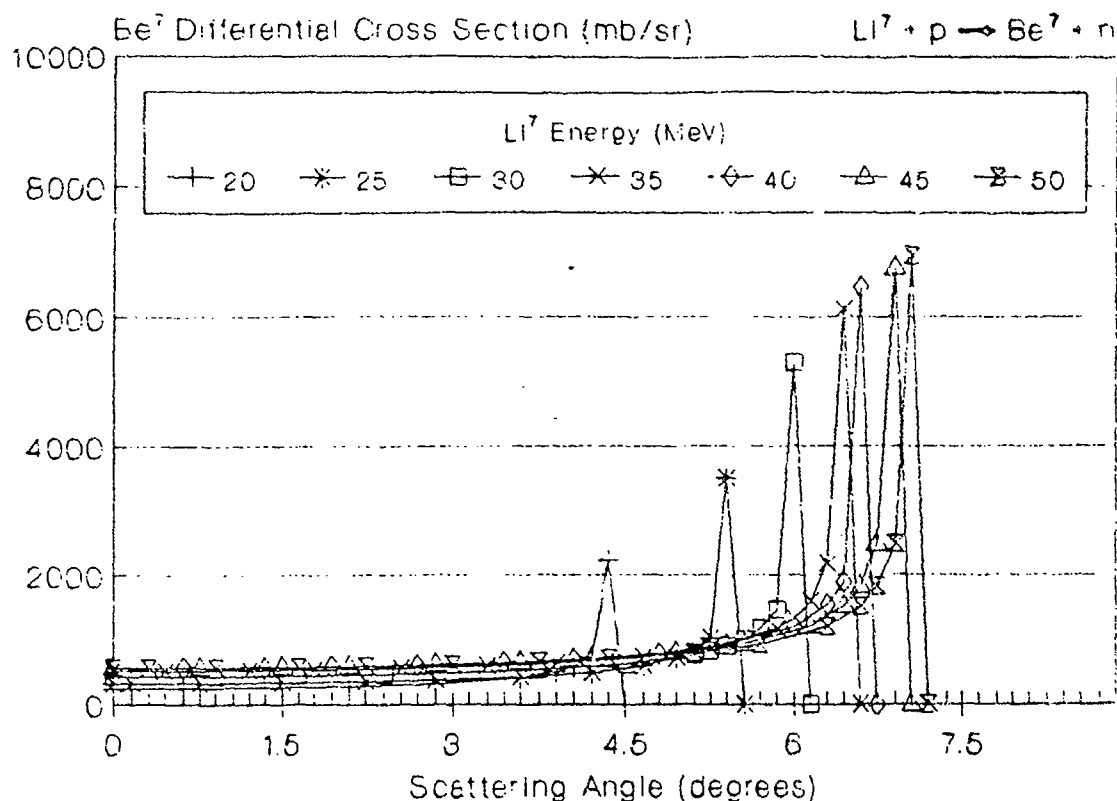


Figure B-3. Differential Cross Section in Lab Coordinates for Several Energies

D. Kinematic Considerations

It has been mentioned that more than one energy is allowed for the recoil scattered atom. This can be seen in Figure B-4, which relates center-of-mass and laboratory particle velocities. This effect occurs whenever $V_{cm} > V_{recoil,cm}$. There is also a critical angle, $\theta_{critical}$, which was given in equation 7, for which only a single V_{lab} recoil can exist. The Lab energy of the recoil at the critical angle is given by (13)

$$E_{CRIT} = \frac{aB}{(a+A)^2} W_{KI} \cos^2 \theta_{CRIT} \quad (24)$$

and is not necessarily half-way between the maximum and the minimum values of W_B . The maximum/minimum lab energies for the recoil atom B are given by the following series of equations where W'_B comes from equation 5.

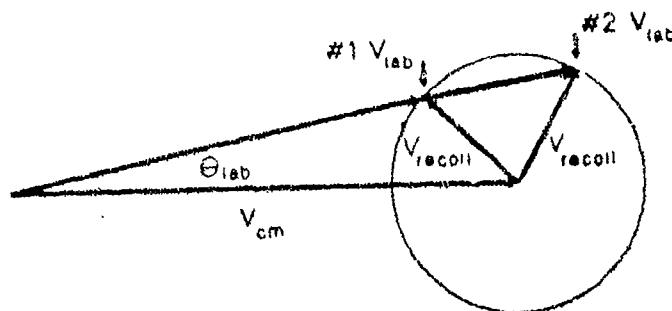
$$W_B = \sqrt{\left(\frac{B V_{LAB}}{C}\right)^2 + B^2 c^4} - \beta c^2 \quad (25)$$

$$W'_{KB} = W'_B - \beta c^2 \quad (26)$$

$$B \frac{V_{LAB}}{C} = \frac{B}{C} (V_{CM} \pm V'_B) \quad (27)$$

$$\begin{aligned} &= \frac{AB}{(a+A)a} \sqrt{(W_{KI} + ac^2)^2 - a^2 c^4} \\ &\quad \pm \sqrt{(W'_{KB} + \beta c^2)^2 - \beta^2 c^4} \end{aligned} \quad (28)$$

It is important to select the kinematic situation in which $V_{cm} > V_B$ because then the scattering angle in the lab cannot be greater than the critical angle. This keeps all of the reaction yield constrained to a small band of scattering angles and greatly improves the rate of accumulation of reaction products.



$$\vec{V}_{cm} = \vec{V}_{lab} + \vec{V}_{recoil}$$

$$V_{cm} > V_{recoil}$$

Figure B-4. Graphical Relationship Between Center-of-Mass and Laboratory Velocities of Recoil Atoms. Note that 2 Center-of-Mass Angles and 2 Lab Velocities are Allowed for 1 Lab Angle.